JACS JOURNAL OF THE AMERICAN CHEMICAL SOCIETY

COMMUNICATION

pubs.acs.org/JACS

Structural and Spectroscopic Characterization of Metastable Thiolate-Ligated Manganese(III)−Alkylperoxo Species

Michael K. Coggins and Julie A. Kovacs*

Department of Chemistry, University of Washington, Seattle, Washington 98195, United States

S Supporting Information

ABSTRACT: Metastable Mn−peroxo species are proposed to form as key intermediates in biological oxidation reactions involving O_2 and C−H bond activation. The majority of these have yet to be spectroscopically characterized, and their inherent instability, in most cases, precludes structural characterization. Cysteinate-ligated metal−peroxos have been shown to form as reactive intermediates in both heme and nonheme iron enzymes. Herein we report the only examples of isolable Mn(III)−alkylperoxo species, and the first two examples of structurally characterized synthetic thiolate-ligated metal−peroxos. Spectroscopic data, including electronic absorption and IR spectra, and ESI mass spectra for ^{16}O vs ^{18}O-labeled metastable Mn(III)−OOR (R = ^tBu, *Cm*) are discussed, as well as preliminary reactivity.

Metastable metal−peroxo species form as key intermediates in biological and biomimetic oxidation reactions involving O_2 and the activation of C−H bonds.[1−16] Manganese−peroxos have been shown to play a significant role in reactions catalyzed by the manganese superoxide dismutase (MnSOD),[17−21] and catalase.[22] A manganese−peroxo dimer is proposed to form in class Ib ribonucleotide reductase (Ib RNR),[23] as well as in the step preceding O_2 evolution by photosystem II (PS II).[24−27] A manganese−alkylperoxo is proposed to form as a key intermediate in manganese lipoxygenase (MnLO)-promoted fatty-acid oxidation.[28−31] The majority of these biological Mn-intermediates have thus far gone unobserved and therefore have yet to be spectroscopically characterized. Much of our current understanding of the properties of these elusive species has come through spectroscopic and/or computational studies involving small-molecule analogues.[16,32−37] The inherent instability of these intermediates usually precludes structural characterization. Research efforts in our laboratory have specifically focused upon the isolation and characterization of thiolate-ligated metal−peroxo species.[38−41] Cysteinate-ligated metal−peroxos have been shown to form as reactive intermediates in the activation of O_2, or derivatives thereof, in both heme (cytochrome P450, chloroperoxidase) and nonheme (superoxide reductase, cysteine dioxygenase) iron enzymes.[6,39,42−44] Herein we report the first two examples of structurally characterized synthetic thiolate-ligated metal−peroxo species, and the only examples of isolable Mn(III)−alkylperoxo species. Spectroscopic data, including electronic absorption and IR spectra, and ESI mass spectra for ^{16}O vs ^{18}O-labeled Mn(III)−OOR (*R* = tBu, *Cm*) are discussed, as well as preliminary reactivity.

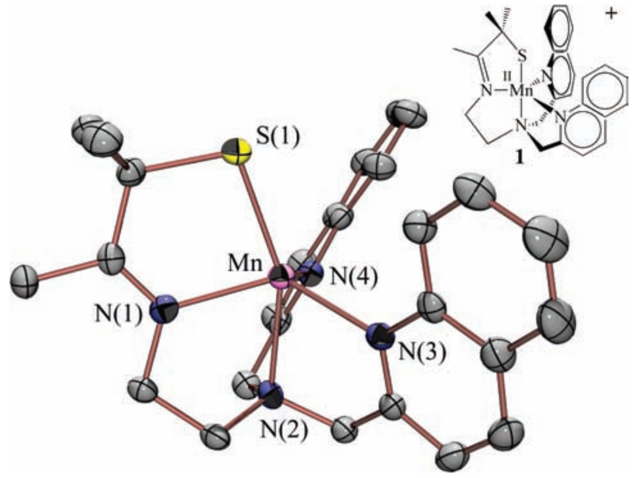

Figure 1. ORTEP and ChemDraw diagram of $[Mn^{II}(S^{Me2}N_4(QuinoEN))]^+$ (**1**) with hydrogen atoms omitted for clarity. Selected metrical parameters (Å): Mn−S(1), 2.3835(9); Mn−N(1), 2.170(2); Mn−N(2), 2.274(2); Mn−N(3), 2.225(3); Mn−N(4), 2.200(3).

Single crystals of our highly reactive and O_2-sensitive Mn(II) complex, $[Mn^{II}(S^{Me2}N_4(QuinoEN))](PF_6)$ (**1**), were obtained *via* ambient temperature vapor diffusion of Et_2O into a saturated MeCN solution. As shown in the ORTEP diagram of Figure 1, the Mn(II) ion of **1** is found in a tetragonally distorted trigonal bipyramidal geometry ($\tau = 0.55$)[45] with an alkyl thiolate sulfur cis to an open coordination site. Metrical parameters, a multiline X-band EPR spectrum (*A* = 91 G; Figure S1), and magnetic susceptibility data ($\mu_{eff} = 5.78\ \mu_B$ (solid state; Figure S2), $\mu_{eff} = 5.83\ \mu_B$ (CH_2Cl_2 solution)) are consistent with a high-spin ($S = 5/2$) ground state. The electronic absorption spectrum of **1** (Figure S3) is featureless throughout the visible region in a variety of solvents (DCM, MeCN, THF, MeOH), also consistent with high-spin Mn(II)

Thiolate-ligated **1** (E_{pa}= +592 mV, E_{pc}= +312 mV vs SCE; Figure S4) reacts immediately with ROOH (R = ^tBu, cumyl) in the presence of 2.0 equiv of triethylamine at −15 °C in CH_2Cl_2 to afford bright blue metastable species, **2a** and **2b**, characterized by absorption bands at λ_{max} = 590 nm (460 $M^{-1}\ cm^{-1}$; Figure 2) and 596 nm (679 $M^{-1}\ cm^{-1}$), respectively. Between 1.5 and 1.8 equiv of ROOH per equivalent of **1** were found necessary to maximize the growth of these absorption bands (Figure 2), and this was shown to be coincident with the complete disappearance

Received: June 21, 2011
Published: July 21, 2011

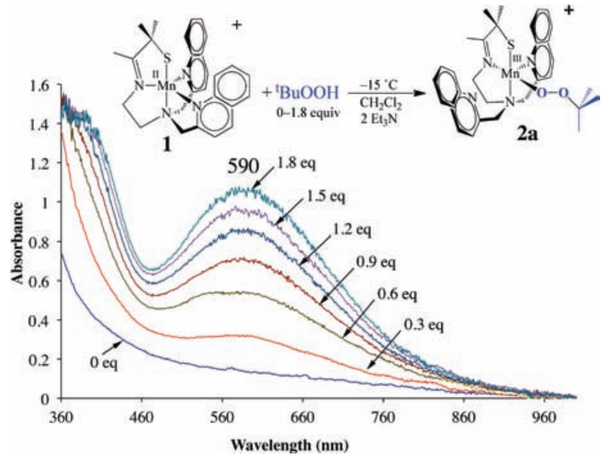

Figure 2. Anaerobic reaction between $[\mathrm{Mn^{II}(S^{Me2}N_4(QuinoEN))}](\mathrm{PF_6})$ (**1**, 2.4 mM) and 1.8 equiv of tBuOOH (0.1 M stock solution; added in 0.3 equiv aliquots) monitored by electronic absorption spectroscopy in CH_2Cl_2 at −15 °C.

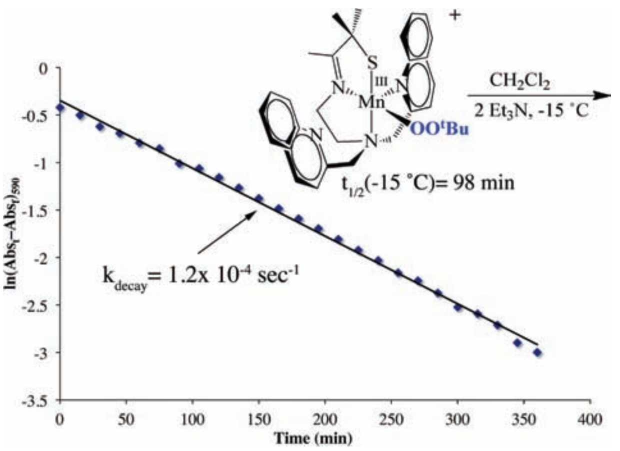

Figure 3. First order kinetics for the decay of $[\mathrm{Mn^{III}(S^{Me2}N_4(QuinoEN))(OOtBu)}]^+$ (**2a**) in the presence of base (Et_3N) monitored by electronic absorption spectroscopy (at λ= 590 nm) in CH_2Cl_2 at −15 °C.

of the X-band EPR signal of **1**. Although the formation of these metastable species does not appear to be influenced by the presence of base (Figure 3, and Figures S5−S7), their lifetimes (at −15 °C) are increased by nearly an order of magnitude when base is present [$\tau_{1/2}$(**2a**, with base) = 5.9(1.7) × 10^3 s,[46] $\tau_{1/2}$(**2a**, without base) = 7.2(2.4) × 10^2 s; Figure 3, Figure S5]. These rates were unaffected by the addition of high excess amounts (100 equiv) of substrates known to react with metal-based oxidants,[47] suggesting that **2a** is incapable of directly oxidizing substrates. Similarly, Nam and co-workers have found $[\mathrm{(tpa)Fe^{III}(OOtBu)}]^{2+}$ to be unreactive with oxidizable substrates.[48] The decay of **2a** and **2b** was also found to be insensitive to O_2, consistent with the complete oxidation of **1**. Upon either warming or prolonged standing in solution over the course of a few hours at −15 °C (Figures 3, and S5−S7), **2a** and **2b** each convert to unstable EPR-silent products.

The vibrational spectrum (FT-IR) of solid samples of **2a**, obtained *via* precipitation from MeCN with cold Et_2O (xs) at −40 °C, displays an isotopically sensitive feature at 888 cm^{-1}, which shifts to 831 cm^{-1} upon ^{18}O-substitution[49] using $^tBu^{18}O^{18}OH$ (Figure 4).

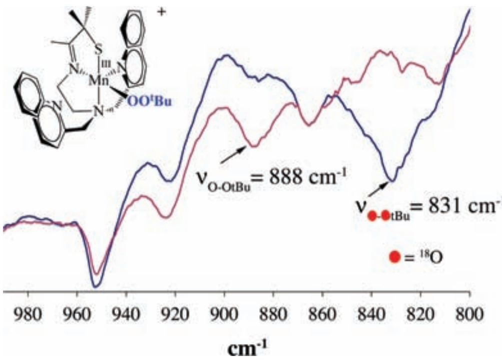

Figure 4. FT-IR spectrum (Nujol) of $[\mathrm{Mn^{III}(S^{Me2}N_4(QuinoEN))(OOtBu)}](\mathrm{BPh_4})$ (**2a**) showing the isotopically sensitive ($^{16}O-^{16}O^tBu$ vs $^{18}O-^{18}O^tBu$) alkylperoxo stretches.

This vibrational frequency is within the expected energy range (750−900 cm^{-1}) for a peroxo ν(O−O) stretch,[3,7,34,35,50,51] and the observed isotopic shift ($\Delta\nu$(exp) = 57 cm^{-1}) is very close to that predicted based upon a harmonic oscillator approximation ($\Delta\nu$(calc) = 51 cm^{-1}). ESI-MS data (Figure S8) is also consistent with a Mn(III)−alkylperoxo species with a mass-to-charge ratio of 585.2 (m/z(calc) = 585.1) that shifts by approximately 4 mass units to m/z = 589.1 upon ^{18}O-incorporation.

Unambiguous identification of the putative metastable Mn(III)−alkylperoxo species was provided by structural determination *via* X-ray crystallography. Exchange of the counterion of **1** from PF_6^- to BPh_4^- permitted us to obtain single crystals of $[\mathrm{Mn^{III}(S^{Me2}N_4(QuinoEN))(OOtBu)}](\mathrm{BPh_4})$ (**2a**) suitable for X-ray diffraction studies in ~60% yield from MeCN/Et_2O (1:5) at −30 °C. We also obtained X-ray-quality crystals of **2b** under similar conditions; however, the resulting structure was solved at lower resolution (R = 16%). Although the metrical parameters are less reliable, the structure of $[\mathrm{Mn^{III}(S^{Me2}N_4(QuinoEN))(OOCm)}](\mathrm{BPh_4})$ (**2b**) does indeed confirm the proposed structure of, and connectivity for, a Mn(III)−alkylperoxo species. The ORTEP diagrams of **2a** and **2b** are provided along with selected metrical parameters in Figures 5 and 6, respectively. Contraction of the Mn−S distance from 2.3835(9) Å in **1** to 2.270(3) Å in **2a** clearly reflects an increase in metal oxidation state from +2 to +3. The solution (CH_2Cl_2) magnetic moments, (μ_{eff}(**2a**) = 4.85(4) B.M., μ_{eff}(**2b**) = 4.81(9) B.M.), are also consistent with oxidized Mn(III) in a high (S = 2) spin-state. Elongation of the Mn−N(1), Mn−N(3), and Mn−N(4) distances in **2a** are most likely a consequence of both the increase in coordination number and Jahn−Teller distortion which would be anticipated for a high-spin Mn(III) ion. In fact, elongation of the Mn−N(4) distance (from 2.200(3) Å in **1** to 2.522(8) Å) in **2a** is so significant that, at least in the solid-state, **2a** is best described as a *five-coordinate* complex with a *dangling quinoline* moiety. The flexibility of the ligand framework in **1** appears to permit the formation of species with more steric congestion around the metal center as is seen in structures **2a** and **2b** (Figure S9).

The Mn−O and O−O bond lengths of **2a**, 1.861(5) and 1.457(7) Å, respectively, are within the expected range for a metal−η^1-alkylperoxo.[52−55] The Mn−O−O angle (109.2(4°)) in **2a** is remarkably acute relative to most metal−alkylperoxo species,[53−55] and similar to that (105.1(2)°) of the only other structurally characterized Mn−alkylperoxo, $\mathrm{Tp^{tBu,iPr}Mn^{II}(O_2CMe_2Ph)}$.[55] This suggests that there is little to no π-bonding interaction between the S = 2 Mn(III) center of **2a** and the

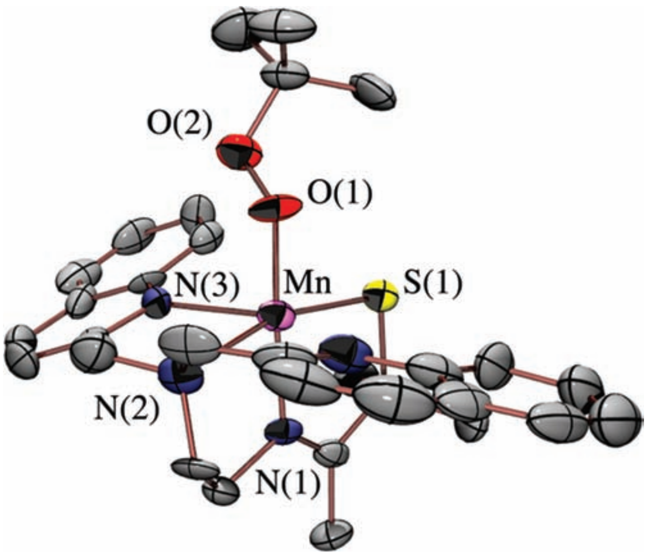

Figure 5. ORTEP of $[\mathrm{Mn^{III}(S^{Me2}N_4(QuinoEN))(OOtBu)}]^+$ (**2a**) with hydrogen atoms omitted for clarity. Selected metrical parameters (Å): Mn−S(1), 2.270(3); Mn−O(1), 1.861(5); O(1)−O(2), 1.457(7); Mn−N(1), 2.034(7); Mn−N(2), 2.173(7); Mn−N(3), 2.349(7); Mn$\cdots$N(4), 2.522(8).

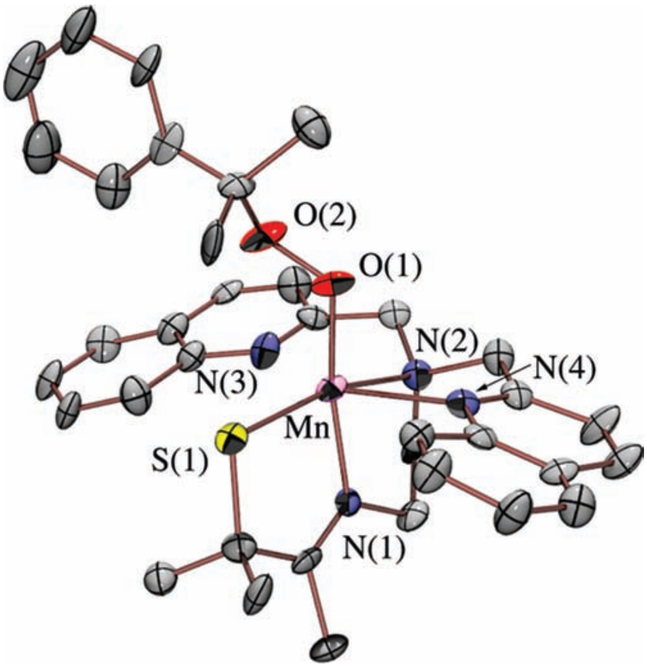

Figure 6. ORTEP of $[\mathrm{Mn^{III}(S^{Me2}N_4(QuinoEN))(OOCm)}]^+$ (**2b**) with hydrogen atoms omitted for clarity. Selected metrical parameters (Å): Mn−S(1), 2.276(5); Mn−O(1), 1.84(1); O(1)−O(2), 1.51(2); Mn−N(1), 2.01(1); Mn−N(2), 2.17(1); Mn$\cdots$N(3), 2.48(1); Mn−N(4), 2.45(1).

proximal peroxide oxygen. One would expect that a lack of multiple bonding interaction between the metal and peroxo oxygen would result in a weaker M−O bond relative to systems in which π-bonding is involved and that this might favor M−O, as opposed to O−O, bond cleavage. GC/MS analysis of the products formed upon warming **2b** to ambient temperature consistently revealed the exclusive production of acetophenone (in 72% yield), as opposed to cumenol. This would suggest that the decay pathway for **2b**, and possibly for **2a** as well, involves O−O bond homolysis.[56] Given the high spin−state of **2b** (and **2a**), this observation contrasts with previous observations regarding the effect of spin-state upon the relative strengths of ferric peroxo M−O and O−O bonds, where high-spin states were seen to favor M−O, as opposed to O−O bond cleavage.[57,58] Similarly, Goldberg and co-workers have reported[59,60] low−spin (S = 1/2) Fe(III)−OOR (R = tBu, Cm) complexes which have low $\nu_{\mathrm{Fe-O}}$ frequencies and force constants (k) that correlate with the donor ability of the *trans*-thiolate ligand, suggesting that they would preferentially undergo Fe−O bond cleavage despite theoretical predictions.

In conclusion, we have described the first two examples of structurally characterized thiolate-ligated metal−peroxo species, and the only examples of isolable Mn(III)−alkylperoxo species. Manganese(III)−peroxos are proposed to be key reactive intermediates in a number of manganese-containing metalloenzyme-promoted reactions. In order to gain insight regarding the mechanism by which **2a** and **2b** decay, both in the presence and absence of substrate, we are currently examining the temperature-dependent kinetics of these reactions. Ideally, these studies will provide insight into the factors that influence O−O versus M−O bond cleavage in small-molecule transition-metal peroxos.

ASSOCIATED CONTENT

Ⓢ **Supporting Information.** Experimental details. This material is available free of charge via the Internet at http://pubs.acs.org.

AUTHOR INFORMATION

Corresponding Author

kovacs@chem.washington.edu

ACKNOWLEDGMENT

NIH funding (#RO1GM45881-19) is gratefully acknowledged.

REFERENCES

(1) Tinberg, C. E.; Lippard, S. J. *Acc. Chem. Res.* **2011**, *44*, 280–288.

(2) Kovaleva, E. G.; Lipscomb, J. D. *Science* **2007**, *316*, 453–456.

(3) Solomon, E. I.; Wong, S. D.; VLiu, L. V.; Decker, A.; Chow, M. S. *Curr. Opin. Chem. Biol.* **2009**, *13*, 99–113.

(4) Rittle, J.; Green, M. T. *Science* **2010**, *330*, 933–937.

(5) Tolman, W. B. *Acc. Chem. Res.* **1997**, *30*, 227–237.

(6) Kuhnel, K.; Derat, E.; Terner, J.; Shaik, S.; Schlichting, I.; Berendzen, J.; Chu, K.; Stock, A. M.; Maves, S. A.; Benson, D. E.; Sweet, R. M.; Ringe, D.; Petsko, G. A.; Sligar, S. G. *Proc. Natl. Acad. Sci. U.S.A.* **2007**, *104*, 99–104.

(7) Li, F.; Meier, K. K.; Cranswick, M. A.; Chakrabarti, M.; Van Heuvelen, K. M.; Munck, E.; Que, L., Jr. *J. Am. Chem. Soc.* **2011**, *133*, 7256–7259.

(8) Fukuzumi, S.; Kotani, H.; Prokop, K. A.; Goldberg, D. P. *J. Am. Chem. Soc.* **2011**, *133*, 1859–1869.

(9) Groves, J. T.; Watanabe, Y.; McMurry, T. J. *J. Am. Chem. Soc.* **1983**, *105*, 4489–4490.

(10) Jin, N.; Ibrahim, M.; Spiro, T. G.; Groves, J. T. *J. Am. Chem. Soc.* **2007**, *129*, 12416–12417.

(11) Prokop, K. A.; de Visser, S. P.; Goldberg, D. P. *Angew. Chem., Int. Ed.* **2010**, *49*, 5091–5095.

(12) Parsell, T. H.; Behan, R. K.; Green, M. T.; Hendrich, M. P.; Borovik, A. S. *J. Am. Chem. Soc.* **2006**, *128*, 8728–8729.

(13) Arunkumar, C.; Lee, Y.-M. M.; Lee, J. Y.; Fukuzumi, S.; Nam, W. *Chem.—Eur. J.* **2009**, *15*, 11482–11489.

(14) Annaraj, J.; Cho, J.; Lee, Y.-M.; Kim, S. Y.; Latifi, R.; de Visser, S. P.; Nam, W. *Angew. Chem., Int. Ed.* **2009**, *48*, 4150–4153.

(15) Lee, J. Y.; Lee, Y.-M.; Kotani, H.; Nam, W.; Fukuzumi, S. *Chem. Commun.* **2009**, 704–706.

(16) Seo, M. S.; Kim, J. Y.; Annaraj, J.; Kim, Y.; Lee, Y.-M.; Kim, S.-J.; Nam, W. *Angew. Chem., Int. Ed.* **2007**, *46*, 377–380.

(17) Bull, C.; Niederhoffer, E. C.; Yoshida, T.; Fee, J. A. *J. Am. Chem. Soc.* **1991**, *113*, 4069–4076.

(18) Abreu, I. A.; Cabelli, D. *Biochim. Biophys. Acta* **2010**, *1804*, 263–274.

(19) Barnese, K.; Sheng, Y.; Stich, T.; Gralla, E. B.; Britt, R. D.; Cabelli, D.; Valentine, J. S. *J. Am. Chem. Soc.* **2010**, *132*, 12525–12527.

(20) Miller, A. F. *Acc. Chem. Res.* **2008**, *41*, 501–510.

(21) Grove, L. E.; Xie, J.; Yikilmaz, E.; Miller, A. F.; Brunold, T. C. *Inorg. Chem.* **2008**, *47*, 3978–3992.

(22) Wu, A. J.; Penner-Hahn, J. E.; Pecoraro, V. L. *Chem. Rev.* **2004**, *104*, 903–938.

(23) Boal, A. K.; Cotruvo, J. A., Jr.; Stubbe, J.; Rosenzweig, A. C. *Science* **2010**, *329*, 1526–1530.

(24) Umena, Y.; Kawakami, K.; Shen, J.-R.; Kamiya, N. *Nature* **2011**, *473*, 55–60.

(25) McEvoy, J. P.; Brudvig, G. W. *Chem. Rev.* **2006**, *106*, 4455–4483.

(26) Betley, T. A.; Surendranath, Y.; Childress, M. V.; Alliger, G. E.; Fu, R.; Cummins, C. C.; Nocera, D. G. *Philos. Trans. R. Soc. London, Ser. B* **2008**, *363*, 1293–1303.

(27) Yachandra, V. K.; Sauer, K.; Klein, M. P. *Chem. Rev.* **1996**, *96*, 2927–2950.

(28) Skrzypczak-Jankun, E.; Bross, R. A.; Carroll, R. T.; Dunham, W. R.; Funk, M. O. *J. Am. Chem. Soc.* **2001**, *123*, 10814–10820.

(29) Oliw, E. H.; Jerneren, F.; Hoffmann, I.; Sahlin, M.; Garscha, U. *Biochim. Biophys. Acta* **2011**, *1811*, 138–147.

(30) Hamberg, M.; Su, C.; Oliw, E. *J. Biol. Chem.* **1998**, *273*, 13080–13088.

(31) Goldsmith, C. R.; Cole, A. P.; Stack, T. D. P. *J. Am. Chem. Soc.* **2005**, *127*, 9904–9912.

(32) Geiger, R. A.; Chattopadhyay, S.; Day, V. W.; Jackson, T. A. *J. Am. Chem. Soc.* **2010**, *132*, 2821–2831.

(33) Shook, R. L.; Peterson, S. M.; Greaves, J.; Moore, C.; Rheingold, A. L.; Borovik, A. S. *J. Am. Chem. Soc.* **2011**, *133*, 5810–5817.

(34) Shook, R. L.; Gunderson, W. A.; Greaves, J.; Ziller, J. W.; Hendrich, M. P.; Borovik, A. S. *J. Am. Chem. Soc.* **2008**, *130*, 8888–8889.

(35) Kitajima, N.; Komatsuzaki, H.; Hikichi, S.; Osawa, M.; Moro-oka, Y. *J. Am. Chem. Soc.* **1994**, *116*, 11596–11597.

(36) Bossek, U.; Weyhermuller, T.; Wieghardt, K.; Nuber, B.; Weiss, J. *J. Am. Chem. Soc.* **1990**, *112*, 6387–6388.

(37) VanAtta, R. B.; Strouse, C. E.; Hanson, L. K.; Valentine, J. S. *J. Am. Chem. Soc.* **1987**, *109*, 1425–1434.

(38) Nam, E.; Alokolaro, P. E.; Swartz, R. D.; Gleaves, M. C.; Pikul, J.; Kovacs, J. A. *Inorg. Chem.* **2011**, *50*, 1592–1602.

(39) Kovacs, J. A.; Brines, L. M. *Acc. Chem. Res.* **2007**, *40*, 501–509.

(40) Kitagawa, T.; Dey, A.; Lugo-Mas, P.; Benedict, J.; Kaminsky, W.; Solomon, E.; Kovacs, J. A. *J. Am. Chem. Soc.* **2006**, *128*, 14448–14449.

(41) Shearer, J.; Scarrow, R. C.; Kovacs, J. A. *J. Am. Chem. Soc.* **2002**, *124*, 11709–11717.

(42) Katona, G.; Carpentier, P.; Nivière, V.; Amara, P.; Adam, V.; Ohana, J.; Tsanov, N.; Bourgeois, D. *Science* **2007**, *316*, 449–453.

(43) Sono, M.; Roach, M. P.; Coulter, E. D.; Dawson, J. H. *Chem. Rev.* **1996**, *96*, 2841–2887.

(44) Aluri, S.; Visser, S. P. *J. Am. Chem. Soc.* **2007**, *129*, 14846–14847.

(45) Addison, A. W.; Rao, T. N.; Reedijk, J. *J. Chem. Soc., Dalton Trans.* **1984**, 1349–1356.

(46) This number represents the average of three runs with the standard deviation shown in parentheses. Figure 3 shows one of three runs.

(47) Substrates examined included acetaldehyde, thioanisole, cyclohexene, cyclooctene, tetracyanoethylene, TEMPO-H, and 2,4,6-tri-*tert*-butylphenol, and 2,4-di-*tert*-butylphenol.

(48) Seo, M. S.; Kamachi, T.; Kouno, T.; Murata, K.; Park, M. J.; Yoshizawa, K.; Nam, W. *Angew. Chem., Int. Ed.* **2007**, *46*, 2291–2294.

(49) Walling, C.; Buckler, S. A. *J. Am. Chem. Soc.* **1955**, *77*, 6032–6038.

(50) Mak, P. J.; Denisov, I. G.; Victoria, D.; Makris, T. M.; Deng, T.; Sligar, S. G.; Kincaid, J. R. *J. Am. Chem. Soc.* **2007**, *129*, 6382–6283.

(51) Roelfes, G.; Vrajmasu, V.; Chen, K.; Ho, R. Y. N.; Rohde, J.-U.; Zondervan, C.; la Crois, R. M.; Schudde, E. P.; Lutz, M.; Spek, A. L.; Hage, R.; Feringa, B. L.; Münck, E.; Que, L., Jr. *Inorg. Chem.* **2003**, *42*, 2639–2653.

(52) Stasser, J.; Namuswe, F.; Kasper, G. D.; Jiang, Y.; Krest, C. M.; Green, M. T.; Penner-Hahn, J.; Goldberg, D. P. *Inorg. Chem.* **2010**, *49*, 9178–9190.

(53) Kitajima, N.; Katayama, T.; Fujisawa, K.; Iwata, Y.; Moro-oka, Y. *J. Am. Chem. Soc.* **1993**, *115*, 7872–7873.

(54) Chavez, F. A.; Mascharak, P. K. *Acc. Chem. Res.* **2000**, *33*, 539–545.

(55) Komatsuzaki, H.; Sakamoto, N.; Satoh, M.; Hikichi, S.; Akita, M.; Moro-oka, Y. *Inorg. Chem.* **1998**, *37*, 6554–6555.

(56) Avila, D. V.; Brown, C. E.; Ingold, K. U.; Lusztyk, J. *J. Am. Chem. Soc.* **1993**, *115*, 466–470.

(57) Lehnert, N.; Ho, R. Y. N.; Que, L. J.; Solomon, E. I. *J. Am. Chem. Soc.* **2001**, *123*, 12802–12816.

(58) Lehnert, N.; Ho, R. Y. N.; Que, L. J.; Solomon, E. I. *J. Am. Chem. Soc.* **2001**, *123*, 8271–8290.

(59) Namuswe, F.; Kasper, G. D.; Narducci Sarjeant, A. A.; Hayashi, T.; Krest, C. M.; Green, M. T.; Moenne-Loccoz, P.; Goldberg, D. P. *J. Am. Chem. Soc.* **2008**, *130*, 14189–14200.

(60) Namuswe, F.; Hayashi, T.; Jiang, Y.; Kasper, G. D.; Narducci Sarjeant, A. A.; Moënne-Loccoz, P.; Goldberg, D. P. *J. Am. Chem. Soc.* **2010**, *132*, 157–167.